Applications of the extended Boltzmann-Uehling-Uhlenbeck model to participant and spectator dynamics

H. H. Gan, S. J. Lee, and S. Das Gupta
Physics Department, McGill University, Montreal, Quebec, Canada H3A 2T8
(Received 28 May 1987)

The Boltzmann-Uehling-Uhlenbeck model is extended to include fluctuations. The model is then applied to study both spectator and participant physics. The model is capable of providing a unified, parameter-free description of wide-ranging phenomena in intermediate energy heavy-ion collisions.

I. INTRODUCTION

In this paper, we present some results from a model in which at initial time we have two ions approaching each other; at the end the nuclei break up into fragments moving with different velocities. The model is essentially parameter-free in the sense that the ingredients for the calculation are the nuclear mean field and scattering cross sections which are fixed by other data.

The model allows us to examine theoretically many aspects of heavy ion collisions. Experience at Bevalac energy has taught us that for nonzero impact parameters we expect to see spectators which are only mildly perturbed as opposed to participants which are at the seat of violent collisions. As the beam energy decreases such clear distinction ultimately will vanish. Our model allows us to study this transition region. We are able to calculate the velocity distribution of the spectators and their slowing down in a fully microscopic model. Likewise we are also able to study, simultaneously, the fragmentation of the participants. This last topic has become the subject of much study in recent years. The model gives a mass distribution; for reasons to be explained later, quantitative fits, isotope by isotope, are not expected. Nonetheless gross features are expected to emerge. At the very least, the model is useful for understanding the change of dynamics as the beam energy is altered. In the present study we have analyzed ^{20}Ne on ^{20}Ne and ^{40}Ca on ^{40}Ca in the energy range 50–100 MeV/nucleon.

The model is a straightforward generalization of the Boltzmann-Uehling-Uhlenbeck (BUU) model[1,2] which has proven to be very useful in the theoretical analysis of heavy ion collisions.

II. THE EXTENDED BUU MODEL

The work presented here is based on the model reported in Ref. 3 except for some changes. We first need to describe some details of the numerical methods to solve the BUU model before we can explain the modifications needed for the extended version. The mean field is taken to be of the form

$$U(\rho)=[-124(\rho/\rho_0)+70.5(\rho/\rho_0)^2]\ \text{MeV} . \quad (1)$$

The collision cross section between nucleons is taken to be 40 mb,[3] although we have also used energy dependent total cross sections to ascertain if any significant differences would be seen. There were none. In the usual BUU model, the initial phase space density is represented by a large number of test particles. If the nucleus A has nucleon number N_A then we represent the initial phase-space density of this nucleus by $N_A\tilde{N}$ test particles. Similarly the phase-space density of the nucleus B is represented by $N_B\tilde{N}$ test particles. For Ne on Ne we take $\tilde{N}=200$; for Ca on Ca we take $\tilde{N}=100$. Each test particle carries an isospin index. The density is defined in cubes of volume 1 fm^3; $\rho(r)=n/(\delta l)^3\tilde{N}$ where n is the number of test particles in the cube and $\delta l=1$ fm. In the BUU model the test particles propagate in time according to $\dot{\mathbf{p}}(t)=-\nabla_r U$ and $\dot{\mathbf{r}}(t)=\mathbf{p}/m$ except when they collide. This collision cross section is $\sigma_{nn}/\tilde{N}$. The Pauli blocking is checked for each collision. When two test particles collide they change from $(\mathbf{r}_1,\mathbf{p}_1)(\mathbf{r}_2,\mathbf{p}_2)$ to $(\mathbf{r}_1,\mathbf{p}_1')(\mathbf{r}_2,\mathbf{p}_2')$. We build a sphere of radius r around $\mathbf{r}_1$ and radius p around $\mathbf{p}_1'$ such that eight test particles in this phase space volume imply complete filling. Define $f_1=n_1/(8-1)$, where n_1 is the number of test particles not including the test particle at $(\mathbf{r}_1,\mathbf{p}_1')$. Similarly $f_2=n_2/7$. The probability of scattering is taken to be $(1-f_1)(1-f_2)$. For low beam energy we have also sometimes used the following preselection rule. Let $\pm\mathbf{p}_0$ be the beam momentum per particle in the c.m. of colliding ions. In a collision we have $\mathbf{p}_1+\mathbf{p}_2=\mathbf{p}_1'+\mathbf{p}_2'$ and $p_1^2+p_2^2=p_1'^2+p_2'^2$. For 1 and 2 to be thrown out of the two Fermi spheres we need $(\mathbf{p}_1'\pm\mathbf{p}_0)^2\geq p_F^2$ and $(\mathbf{p}_2'\pm\mathbf{p}_0)^2\geq p_F^2$. Using the conservation laws, a necessary (but by no means sufficient) condition for this to happen is

$$(\mathbf{p}_1\pm\mathbf{p}_0)^2+(\mathbf{p}_2\pm\mathbf{p}_0)^2>2p_F^2 .$$

At high energy this is not a good rule as it neglects the depletion in the Fermi sphere, but at low energy we find this is a useful preselection and cuts down on computing. Once the preselection rule is satisfied the test particles are allowed to scatter; afterwards the Pauli blockings for $\mathbf{p}_1'$ and $\mathbf{p}_2'$ are tested by drawing spheres in phase space as described earlier. The numbers of collisions we

find in our calculation are consistent with what has appeared in the literature before.[3,4]

The BUU model treats collisions as a continuous source and will show no fluctuations. In the extended BUU model collision is treated stochastically. The following is the basic prescription. We suppress collisions between two test particles by a factor of $1/\tilde{N}$, but if a collision occurs after the suppression not only do two test particles suffer momenta change but $2(\tilde{N}-1)$ other test particles change momenta also. Physically this corresponds to two actual particles colliding. Suppose two test particles i and j with isospin indices τ_i and τ_j successfully collided and suffered momenta change $\Delta\mathbf{p}$ and $-\Delta\mathbf{p}$. We choose $(\tilde{N}-1)$ test particles with the same isospin τ_i closest to i in phase space and ascribe to all of them the same momentum change $\Delta\mathbf{p}$. This requires defining a distance in phase space. We define

$$d_{ik}^2 \propto (\mathbf{p}_i-\mathbf{p}_k)^2+(p_F/R)^2(\mathbf{r}_i-\mathbf{r}_k)^2 \ .$$

Here p_F is the Fermi momentum and R the normal radius of the nucleus. The process is repeated for test particles closest to j and they are ascribed a momentum change $-\Delta\mathbf{p}$.

The prescription above conserves total momentum but usually not the total energy. With a slight modification both the total momentum and the total energy can be conserved. We choose $\tilde{N}-1$ particles closest to i as before. Now calculate the average momentum of these particles (including the ith test particle). Call this

$$\langle \mathbf{p}_i \rangle \equiv \left[\sum_{i=1}^{\tilde{N}} \mathbf{p}_i \right] / \tilde{N} \ ;$$

similarly calculate $\langle \mathbf{p}_j \rangle$. We now recalculate $\Delta\mathbf{p}$ and $-\Delta\mathbf{p}$ from a collision between $\langle \mathbf{p}_i \rangle$ and $\langle \mathbf{p}_j \rangle$. This $\Delta\mathbf{p}$ is now attributed to all the test particles in the ith set and $-\Delta\mathbf{p}$ to all the particles in the jth set. It is easy to verify that this procedure conserves both total momentum and total energy.

We have done calculations both with and without the Coulomb force. We compute $\rho_c(\mathbf{r})$ in 1 fm^3 boxes where $\rho_c(\mathbf{r})$ is the charge density. The Coulomb potential is then obtained from numerical solution of Poisson's equation. The numerical technique is the same as used in time dependent Hartree-Fock (TDHF) calculations[5] except that in our case no symmetry is assumed.

In the beginning of the calculation we have two nuclei approaching each other; the initial phase-space density of each nucleus is modeled to be sharp spheres in configuration and momentum space. For further details, see the Appendix of Ref. 6. At the end one has a few local pockets of density comparable to normal nuclear density against a diffuse background. We interpret such local pockets as clusters. A fragment is defined as the connected volume in space where the density exceeds a certain threshold value (10% of normal nuclear density). The number of nucleons in this connected volume gives the number of nucleons in the cluster. We ignore all clusters where the total nucleon number is less than 0.5. Depending upon the situation, the code is run up to time 80–150 fm/c after the two nuclei initially touch each other. On Vax 785 each run takes 45 min without the Coulomb interaction. Inclusion of the Coulomb interaction approximately doubles this time.

III. SPECTATOR DYNAMICS

For heavy ion collisions at high energy, the participant spectator model proved to be very useful. Consider the collision of two heavy ions at a given impact parameter (Fig. 1). A given part A of one ion will meet a certain part B of the other ion. Now the binding energy per nucleon in nuclei is about 8 MeV. Thus if the energy of collision is high, the fact that A' was attached to A is incidental; A' will fly off after the collision with essentially unchanged velocity. Thus A' can be called the spectator in this collision. Similarly there will be a spectator B' from the other ion. A, however, will hit B. They are the participants. The participants will usually disintegrate, giving rise to many objects.

We do not expect such a clear picture to emerge in the energy range we are considering. Clearly, below a certain beam energy the model of the whole of $(A+A')$ interacting with the whole of $(B+B')$ is more appropriate. An intermediate picture between these two extremes is also possible. Further, the applicability of each model depends not only upon the beam energy but also upon the masses of the colliding ions involved. These complications become important at intermediate impact parameters. We will deal with such situations later. For the moment we turn to more peripheral collisions where one clearly sees spectatorlike fragments. Experimental results for projectilelike spectators in the beam energy of interest here can be found in Refs. 7–9.

Comparison with experimental data requires integration over impact parameters and (depending upon the charges of the ions and the beam energy) inclusion of the Coulomb force in addition to the nuclear force. To be able to discuss the physics easily we will first consider a fixed impact parameter and ignore the Coulomb force.

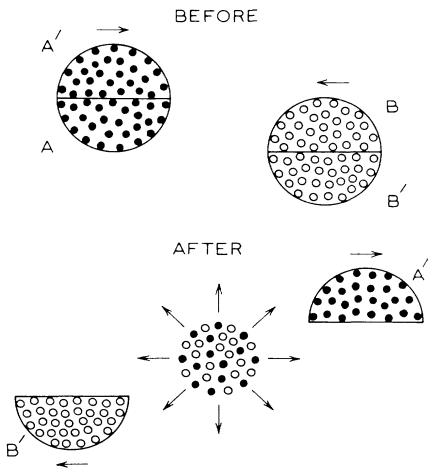

FIG. 1. Participants and spectators. Part A overlaps with part B. They are participants. Parts A' and B' are spectators.

The effect of impact parameter integration and the Coulomb force will be indicated later. We consider Ne on Ne at impact parameter

$$b = R(\sqrt{2/3}+\sqrt{1/3}) = 4.31 \text{ fm}$$

at 100 MeV/nucleon laboratory energy. Here R is the radius of each ion. In a simple geometrical model (Fig. 1) the participants are decided by the geometrical overlap of the two ions; the rest are spectators. There are two spectators; one projectilelike and one targetlike. The number of nucleons in each spectator is predicted to be 16.6 in the geometrical model for this specific b. In a dynamical model one would expect a distribution in mass numbers. The distribution obtained from 21 runs is shown in Fig. 2. Each run produces two pieces of data since we are considering equal ion collisions and we can include both projectilelike and targetlike spectators to increase statistics. The spectators have a distribution of momenta. In the Goldhaber model[10] the width of this momentum spread in the projectile frame is

$$\langle P_{ZK}^2 \rangle = \frac{K(A-K)}{A-1}\sigma_{\parallel}^2 . \tag{2}$$

Here A is the mass of the projectile, K is the mass of the spectator, P_{ZK} is the momentum of the spectator in the Z direction in the projectile frame, and $\sigma_{\parallel}=\sigma_Z \approx 80$ MeV/c in the high energy situation.

In our case we have a distribution of K values and we find it more convenient to rewrite the above equation

$$\left\langle \frac{K(A-1)}{A-K}(P_{ZK}/K - \overline{P_{ZK}/K})^2 \right\rangle = \sigma_{\parallel}^2 . \tag{3}$$

Here $\overline{P_{ZK}/K}$ is the average slowing down in the projectile frame. The Goldhaber model is based solely on counting and thus cannot predict a slowing down. However, this is expected in dynamical models and also seen in experiments. We expect $\overline{P_{ZK}/K}$ to be independent of K but dependent on b, the impact parameter. Hence for this fixed b value we calculate $\overline{P_{ZK}/K}$ from all K values and use this in Eq. (3) to estimate $\sigma_{\parallel}$. We find $\sigma_{\parallel} \approx 70$ MeV/c. A decrease in the value of $\sigma_{\parallel}$ at lower energy was predicted on theoretical grounds.[11] The quantity $\overline{P_{ZK}/K}$ is found to be -33 MeV/c compared to the experimental value of -23 MeV/c seen in experiments at 92 MeV/nucleon beam energy.[9] Precise comparison with experiment should not be made at this stage as $\overline{P_{ZK}/K}$ is dependent upon b, the magnitude falling with increasing b.

We digress here temporarily to indicate the numerical accuracy in our calculation. The collision subroutine conserves momenta and energy. The only inaccuracy in our calculations is in solving the Vlasov propagation. This was tested by calculating conserved quantities for an isolated nucleus at time $t=0$ and $t=100$ fm/c at which time the majority of our calculations can be stopped. We have also considered more complicated situations where again one can test conserved quantities. Of interest here is the fluctuation in the total momentum in a direction, say y, and the loss in the number of particles due to numerical inaccuracy in the Vlasov propagation. Both of these effects are small, at a less than 5 percent level of the value of the observables we are trying to calculate.

It is likely that the spectators will also have an average transverse momentum. This, of course, is outside the scope of the Goldhaber model. In our calculation we take b to be in the X direction. It is possible for $\overline{P_{XK}/K} \equiv \bar{p}_X$ to be nonzero. Naturally we expect $\bar{p}_y = 0$. This is borne out in our calculations. In the present example we find $\bar{p}_X = -29.4$ MeV/c. (Similar results have been found by Tsang in BUU calculations.[12]) However, the value of $\bar{p}_X$ is a function of both the impact parameter and the energy. For this energy it has a negative value; the magnitude initially grows with impact parameter, reaches a maximum (near $b=4.31$ fm), and then begins to fall. A net nonzero value of $\bar{p}_X$ will tend to deviate the spectators away from the forward direction. This would imply that $d\sigma/d\Omega$ maximizes not at 0°, but at some finite angle. Relevant experimental data[7–9] indicate that the maxima, if not at 0°, are between 0° and 2°. We will later show that, at this energy, the Coulomb interaction acts the opposite way and integration over impact parameter will push the maximum of $d\sigma/d\Omega$ to-

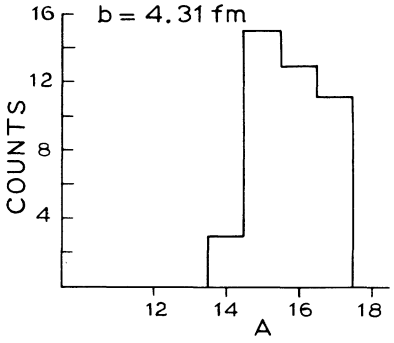

FIG. 2. For Ne on Ne collisions at 100 MeV/nucleon the distribution in masses of the spectators for impact parameter $b=4.31$ fm. The results from 21 runs are shown. Each run gives two spectators.

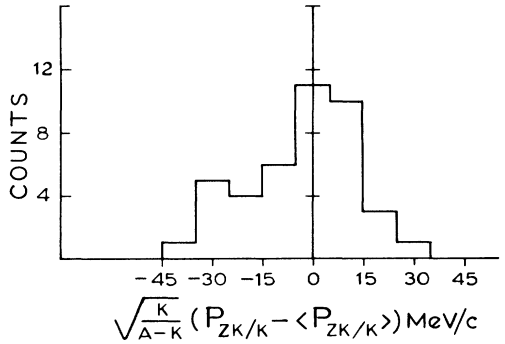

FIG. 3. Distribution of the z component of the momentum of the spectatorlike fragments. The case shown is for Ne on Ne at $b=4.31$ fm; the beam energy is 100 MeV/nucleon.

wards 0°. For the moment, we will continue discussing this one impact parameter and without the Coulomb force.

A formula similar to Eq. (3) can be used to calculate σ_X^2 and σ_Y^2. In this specific case we verify that $\sigma_X^2 \approx \sigma_Y^2 \approx \sigma_Z^2$. One can test if the momentum distribution is Gaussian,

$$\sigma(P_{ZK}) \propto \exp[-(P_{ZK}-\bar{P}_{ZK})^2/2\langle(P_{ZK}-\bar{P}_{ZK})^2\rangle] . \quad (4)$$

A histogram of the distribution seen in the present example is shown in Fig. 3. A Gaussian conjecture appears to be a reasonable approximation, although many more runs are required to establish a shape unambiguously.

Experimentally one usually measures $d^2\sigma/dE\,d\Omega$ for projectilelike fragments at a small angle θ with respect to the beam axis. To calculate this directly in Monte Carlo simulation would take prohibitively long. Instead we extract $\bar{p}_Z$, $\bar{p}_X$, and width from the Monte Carlo simulations and use the Gaussian assumption [Eq. (4)] to compute $d^2\sigma/dE\,d\Omega$. Let θ be the angle the detector makes with respect to the beam axis and $Z-X$ be the plane containing the beam and the detector, then a fragment of momentum $\mathbf{P}_K$ reaching the detector has the following momentum decomposition:

$$\mathbf{P}_K = P_K\cos\theta\hat{Z} + P_K\sin\theta\hat{X} .$$

The cross section for the event is

$$\frac{d^3\sigma}{d^3P_K} \propto \exp[-(\mathbf{P}_K - \bar{P}_{ZK}\hat{Z} - \bar{P}_{\perp K}\hat{n}_\perp)^2/2\sigma_K^2] . \quad (5)$$

In Eq. (5), $\bar{P}_{ZK}$ is the average momentum in the Z direction, $\bar{P}_{\perp K}$ is the average transverse momentum, and $\hat{n}_\perp$ is the direction of the impact parameter which is not known and needs to be averaged. When this is done, Eq. (5) leads to

$$\frac{d^2\sigma}{dE\,d\Omega} \propto E^{1/2}\exp[-(P_K^2+\bar{P}_{ZK}^2+\bar{P}_{\perp K}^2-2P_K\bar{P}_{ZK}\cos\theta)/2\sigma_K^2]\int_0^{2\pi}\exp(2P_K\sin\theta\bar{P}_{\perp K}\cos\theta_1/2\sigma_K^2)d\theta_1/2\pi . \quad (6)$$

The last integral in Eq. (6) is the Bessel function $J_0(-iP_K\sin\theta\bar{P}_{\perp K}/\sigma_K^2)$. In our specific example we choose $K=15$; at $\theta=3.5°$ numerical calculation using Eq. (6) gives a full width at half maximum (FWHM) of 143 MeV. This is to be compared with the value ≈ 160 MeV seen in experiments at 85 MeV/nucleon laboratory energy.[8] Again, since impact parameter integration has not been done, 143 MeV is a rough estimate.

We now return to the discussion of a net $\bar{p}_\perp$ in the spectator. If this is large it signifies a measurable deflection away from the forward direction. (We have verified that at higher energy, 200 MeV/nucleon, the effect is negligible.) We have chosen $b=4.31$ fm, where $p_\perp(b)$ due to nuclear forces is about maximum in magnitude. It has a negative value which implies negative angle scattering. A quantitative estimate of the deflection away from the 0 degree can be obtained by plotting a histogram of the spectator angles as obtained in Monte Carlo simulations directly; alternatively we calculate σ_K^2, $\bar{P}_{ZK}$, and $\bar{P}_{\perp K}$ from our simulations, use these values in Eq. (6), and integrate $\int(d^2\sigma/dE\,d\Omega)dE$ to obtain $d\sigma/d\Omega$ as a function of θ. In Fig. 4 we have done both and obtained the results with and without the Coulomb force. The Coulomb force by itself would impart a positive $p_\perp$ and thus, in this example, brings the maximum closer to 0°.

Several other representative calculations were done which lead us to believe that the model can at least semiquantitatively describe spectator dynamics. We can account for the slowing down of the spectators. In experiments the slowing down per particle is the largest for smaller fragments.[7] This is easily explained in the model; the lighter projectilelike fragments originate from lower impact parameter and the mean field is more effective in decelerating the projectile. We have seen that apart from the Coulomb field, the nuclear mean field, can, by itself, impart a transverse momentum. This depends upon the beam energy but also upon the nuclear masses; this has an important effect on the angular distribution. In the future we will make detailed calculations to compare with all the available experimental data[7-9] in this energy range.

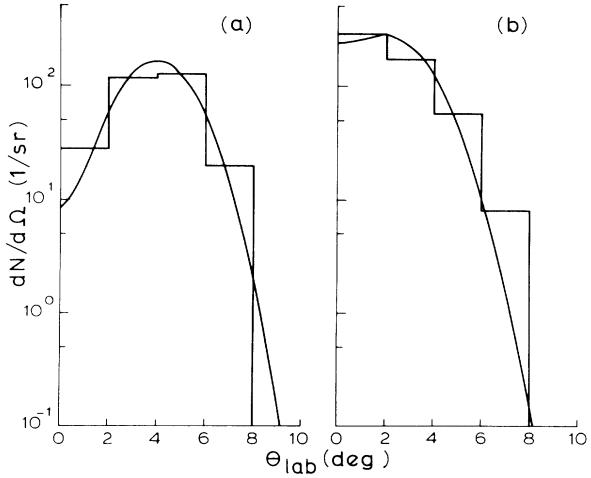

FIG. 4. Distribution in angle for spectatorlike fragments without (a) and with (b) the Coulomb force included. The histograms are obtained by binning the spectator angles as obtained from the runs; the continuous curves are obtained from the Gaussian assumption [Eq. (6)] where the constants σ_K^2, $\bar{P}_{\perp K}$, and $\bar{P}_{ZK}$ are determined from the runs. Here $K=15$.

IV. MASS DISTRIBUTION OF PARTICIPANTS

We now turn to more central collisions and ask the following question: What is the mass distribution of fragments which are not spectatorlike? A variety of approaches have been used to answer this question: microcanonical ensemble simulations,[13–15] the evaporation model,[16] various models of liquid-gas phase transition (see Ref. 17 and references therein), the Cascade-Vlasov approach,[6] and various other models.[18,19]

For central collisions ($b=0$), a mass distribution was obtained in Ref. 3 for Ne on Ne collision at 100 MeV/nucleon in a calculation very similar to the present one. To be able to compare with experimental data we need to integrate over impact parameter. We would also like to see how the theoretical predictions change as the beam energy is varied.

Figure 5 shows our results for Ca on Ca collision at 92 MeV/nucleon. Thirty runs spanning the impact parameter $b=0$ to 4.2 fm were taken. To reduce statistical fluctuations, the results have been averaged over 3 mass units for each bin. Figure 5 gives the histogram of all the clusters and also a filtered histogram where we remove spectatorlike fragments. We use the following criterion: In the c.m. of the colliding ions, the initial momentum per particle in each ion is $\pm p_Z$. After the collision if the absolute value of the Z component of the momentum per particle in the cluster is $> 0.6p_Z$ in the c.m., we leave them out. This means (a) we rule out those projectilelike fragments whose Z component of momentum per particle in the laboratory is greater than $0.8(p_Z)_{\text{lab}}$, and (b) we rule out targetlike spectators which are slowly moving in the lab. For this beam energy this amounts to ruling out targetlike spectators whose kinetic energy in the laboratory is less than ($3.65A$ MeV), where A is the number of nucleons in the cluster.

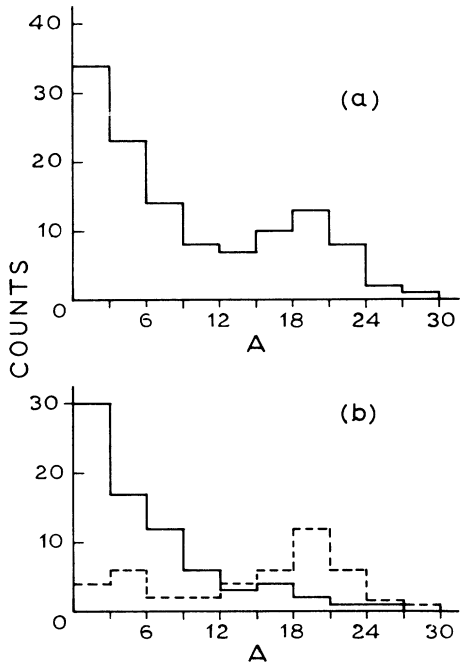

FIG. 5. Mass distributions for Ca on Ca collisions at 92 MeV/nucleon. This is the result from 30 runs spanning the impact parameter b from 0 to 4.2 fm; the top curve (a) includes all clusters; in (b) we separate out contributions from participants (solid line) and spectators (dashed line); for the latter a cut in the momentum of the fragments in the c.m. of the colliding ions is imposed for the distinction. The yield $Y(A)$ given by the solid curve in (b) falls off slower than what is seen in experiment (Ref. 20).

In our calculation (Fig. 5), we see that the yield $Y(A)$ from participants falls off with A with some leveling occurring around $A \approx 12$. There are some recent data obtained in experiments of Ar on Ca at 92 MeV/nucleon.[20] The falloff seen in experiments is faster than what the calculation gives. If we constrain ourselves to fit both the experimental data and the theoretical calculation by a power law $Y(A) \approx A^{-\tau}$, then experiment gives $\tau \approx 3.0$, whereas theory gives $\tau \approx 1.5$. Experimental data do not go beyond $A=12$, but there is some indication of the cross section flattening out around $A \approx 10$. The main failure of the model therefore is that the initial falloff is too slow.

Figure 6 shows results of a similar calculation for Ne on Ne at 100 MeV/nucleon. Here 25 runs spanning $b=0$ to 3.9 fm were taken. In the data shown in Fig. 6 the Coulomb interaction is included; however, for fragmentation of Ca on Ca or Ne on Ne, the Coulomb interaction is unimportant. Remembering that in the latter case the total number of nucleons is half compared to the case for Ca on Ca, the mass distribution in the case of Ne on Ne is similar to that of Ca on Ca.

The model fails at low beam energy. At high energy, the two nuclei, upon impact, quickly break up and nu-

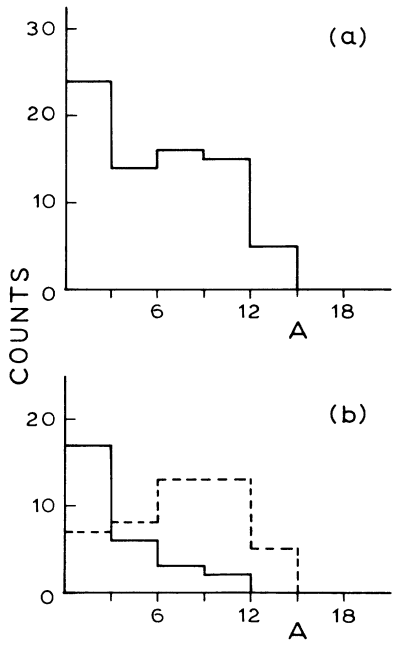

FIG. 6. Same as in Fig. 5 except that we consider Ne on Ne at 100 MeV/nucleon.

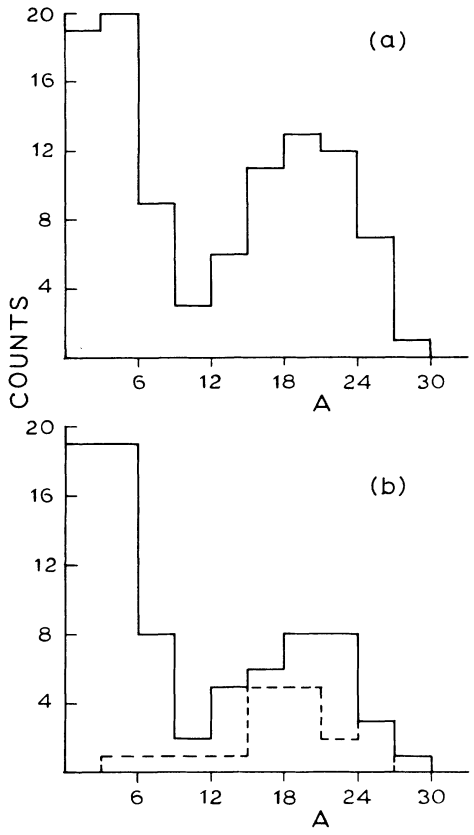

FIG. 7. Same as in Fig. 5 except that this is for Ca on Ca at 72 MeV/nucleon. Note that the yield $Y(A)$ vs A for the participantlike fragments [solid curve in (b)] shows a minimum around $A \approx 12$.

cleons which are close together in phase space will remain bound to produce clusters. At low beam energy the scenario is different; energy is dumped into a region of configuration space but it is not enough to break up the system quickly. Consequently, other processes like evaporation, which cannot be accommodated in the present framework, will become a major mechanism in deciding the mass distribution. A beam energy of 50 MeV/nucleon is already too low for this model.

Figure 7 shows our calculation for Ca on Ca at 72 MeV/nucleon. We have no reason to believe that at this energy the model will break down qualitatively. The most noticeable feature is the U shape of the reaction cross section as a function of A. This shape remains after one removes from the histogram spectatorlike fragments. Recent experimental data[20] have not established this increase of $Y(A)$ vs A beyond $A=12$, but there is at least a hint of this occurring in the experiment[20] of Ar on Ca at 42 MeV/nucleon. Unfortunately the data do not go beyond $A=12$; for equal ion collisions data up to $A \approx 24$ would be a very useful test of the model.

V. SUMMARY AND DISCUSSION

The extended BUU model is a direct generalization of the BUU model which has become a very useful theoretical tool for intermediate energy heavy ion collisions. We therefore felt that it is important to test the predictive power of the extended BUU model. It is a parameter-free model which addresses a very complex problem. It is gratifying to see that the main features of spectator physics come out rather well from the model. In future work we will include the diffuseness of the surface carefully, as one expects this to play a significant role for precise comparison with experiments. Our present treatment does not treat the surface properly. This is related with the larger problem of treating the surface in the Vlasov prescription. For mass distributions in more central collisions between equal ions, the most interesting prediction is that we expect to see a minimum in the $Y(A)$ vs A curve. This should happen between 50 and 100 MeV/nucleon beam energy.

Note added. The average properties of spectators can be studied in the standard BUU model. Recent work can be found in Refs. 21 and 22. We thank C. Grégoire for bringing this to our attention.

ACKNOWLEDGMENTS

S. Das Gupta acknowledges many discussions with G. F. Bertsch. This work was supported in part by NSERC and in part by the Quebec Department of Education.

[1]G. F. Bertsch, H. Kruse, and S. Das Gupta, Phys. Rev. C **29**, 673 (1984).
[2]H. Kruse, B. V. Jacak, and H. Stocker, Phys. Rev. Lett. **54**, 289 (1985).
[3]W. Bauer, G. F. Bertsch, and S. Das Gupta, Phys. Rev. Lett. **58**, 863 (1987).
[4]J. Aichelin and G. F. Bertsch, Phys. Rev. C **31**, 1730 (1985).
[5]S. E. Koonin, K. T. R. Davies, V. Maruhn Rezwani, H. Feldmeier, S. J. Krieger, and J. W. Negele, Phys. Rev. C **15**, 1359 (1977).
[6]S. Das Gupta, C. Gale, J. Gallego, H. H. Gan, and R. D. Ratna Raju, Phys. Rev. C **35**, 556 (1987).
[7]R. Dayras *et al.*, Nucl. Phys. **A460**, 299 (1986).
[8]C. Guet, Nucl. Phys. **A400**, 191C (1983).
[9]K. Van Bibber *et al.*, Phys. Rev. Lett. **43**, 840 (1979).
[10]A. S. Goldhaber, Phys. Lett. **53B**, 306 (1974).
[11]G. F. Bertsch, Phys. Rev. Lett. **46**, 472 (1981).
[12]M. B. Tsang, Nucl. Phys. (to be published).
[13]G. Fai and J. Randrup, Nucl. Phys. **A381**, 557 (1982).
[14]S. E. Koonin and J. Randrup, submitted to Nucl. Phys.
[15]D. H. E. Gross, Nucl. Phys. (to be published).
[16]W. A. Friedman and W. G. Lynch, Phys. Rev. C **28**, 950 (1983).
[17]L. P. Csernai and J. I. Kapusta, Phys. Rep. **131**, 224 (1986).
[18]J. Aichelin and H. Stoecker, Phys. Lett. B **176**, 14 (1986).
[19]G. E. Beauvais, D. H. Boal, and J. C. K. Wong, Phys. Rev. C **35**, 545 (1987).
[20]B. V. Jacak *et al.*, Phys. Rev. C **35**, 1751 (1987).
[21]C. Grégorie, B. Rémaud, F. Sébille, and L. Vinet, Phys. Lett. B **186**, 14 (1987).
[22]A. Bonasera, M. di Toro, and C. Grégoire, Nucl. Phys. **A463**, 653 (1987).